

ORIGINAL RESEARCH PAPER

Enhancement of tetracycline removal in aquatic environment by nano-pyrite//ultrasound as a sono-Fenton process

Elham Aseman-Bashiz¹, Hossein Sayyaf^{1,2}

¹Environmental Health Engineering Lecturer, Alifard (SANICH) Institute of Applied Nscience and Technology, Hashtgerd, Alborz, Iran

²Department of Environmental Health Engineering, Tehran University of Medical Sciences, Health Assistant Department, South Tehran Health Center, Tehran, Iran

Received: 2022-11-10

Accepted: 2023-01-25

Published: 2023-05-22

ABSTRACT

This study was conducted to introduce a new sono-Fenton system containing a nano-pyrite catalyst and hydrogen peroxide (HP) for the effective removal of tetracycline (TC) from aqueous solutions. The synthesized nano-pyrite was characterized through XRD, FTIR, FE-SEM, and EDX analyses. The best performance of the sono-Fenton nano-pyrite/HP system was observed under the condition of pH 3.0, TC 8.0 mg/L, HP 4.0 mM, ultrasound (US) 40 W, nano-pyrite 1.0 g/L, and 20 min with 93.1% removal efficiency. A comparison of the efficiency of the proposed system components confirmed the remarkable synergy between sono-catalysis and Fenton reactions due to the simultaneous application of nano-pyrite, HP, and US power. Meanwhile, US irradiation caused fluidization, turbulence, mass transfer, and nano-pyrite surface cleaning due to its cavitation and oscillation effects. According to the tracer test, the main agent of TC degradation in the sono-Fenton process was HO[•]. The results showed that the TC removal efficiency from the first to the fourth run reached 93.1% to 70.3%. This means that the recyclability of nano-pyrite has been very successful. Overall, the proposed sono-Fenton system was an efficient and sustainable process for the rapid and effective removal of pharmaceutical contaminants from water and wastewater.

Keywords: Hydrogen peroxide; Nano-pyrite; Sono-Fenton; Tetracycline; Ultrasound

How to cite this article

Aseman-Bashiz E., Sayyaf H., Enhancement of tetracycline removal in aquatic environment by nano-pyrite//ultrasound as a sono-Fenton process. J. Water Environ. Nanotechnol., 2023; 8(2): 179-189 DOI: 10.22090/jwent.2023.02.007

INTRODUCTION

Tetracycline (TC) is one of the most medically prescribed antibiotics due to its high effectiveness in treating infections such as cholera, syphilis, and brucellosis. The poor metabolism of TC in the human body causes its excretion into the aquatic environment [1]. TC is an organic pollutant resistant to biodegradation in aqueous solutions, so conventional water and wastewater treatment processes are not able to remove it effectively [2]. In recent years, the use of advanced oxidation processes (AOPs) to remove antibiotics

has been considered. Among AOPs (ozonation, Fenton process, ultraviolet, and electrochemical), the Fenton process is one of the most effective processes for removing organic pollutants [3-5]. In this process, the hydroxyl radical (HO[•]) is produced by the simultaneous use of hydrogen peroxide (HP, H₂O₂) and ferrous ions (Fe²⁺) (Eqs. (1)). Effective oxidation and removal occurs through an attack of HO[•] on the organic pollutant structure [6]. To supply Fe²⁺ in the Fenton process, common iron compounds such as ferrous sulfate (FeSO₄) can be used [7]. Despite the favorable effectiveness, sludge production and high stoichiometric consumption

* Corresponding Authors Email: environmental_sayaf@yahoo.com



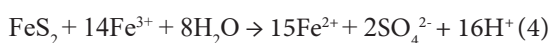
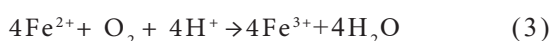
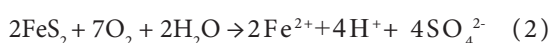
This work is licensed under the Creative Commons Attribution 4.0 International License.

To view a copy of this license, visit <http://creativecommons.org/licenses/by/4.0/>.

of Fe^{2+} are the main disadvantages of the mentioned compound [8, 9]. The use of heterogeneous iron catalysts can overcome these disadvantages [10, 11].



Pyrite (FeS_2) is an abundant heterogeneous iron catalyst in the earth's crust, which has attracted researchers due to its features such as reusability, easy access, non-toxicity, low cost, and regulating the cycle of iron ions in the solution (Eqs. (2-4)) [12, 13].



In addition, it has been proven that the use of nanosizing processes to increase the surface area of the catalyst leads to the improvement of organic pollutant removal [14, 15]. According to previous studies, the use of combined AOPs has improved the efficiency of pharmaceutical removal. In this regard, the use of ultrasonic irradiation (US) in the Fenton process improves the production of $\text{HO}\cdot$ (Eqs. 5). Moreover, the US causes continuous cleaning of the catalyst surface and subsequently improves its performance [16-19].



In the present study, the use of nano-pyrite for the effective activation of HP under ultrasound irradiation was introduced in a novel combined sono-Fenton process. According to our investigations, no study has been done on the use of nano-pyrite in sono-Fenton activation of HP for TC removal from aqueous solutions. In this way, characterization analyses of nano-catalyst were studied. The effect of operational parameters was evaluated. Furthermore, the influence of different processes on TC removal efficiency was compared. Finally, the reusability of synthesized nano-pyrite was presented.

MATERIALS AND METHODS

Chemicals

Tetracycline ($\text{C}_{22}\text{H}_{24}\text{N}_2\text{O}_8$) was purchased from Tolid Daru Pharmaceutical Company, Iran. Hydrogen peroxide, sodium hydroxide (NaOH),

sulfuric acid (H_2SO_4), nitric acid (HNO_3), tert-butanol alcohol ($\text{C}_4\text{H}_{10}\text{O}$), methanol (CH_3OH), and ethanol ($\text{C}_2\text{H}_6\text{O}$) were supplied by Neutron Pharmaceutical Company, Iran. All chemicals were used in pure form.

Preparation of nano-pyrite

Pure pyrite powder was obtained from the Faculty of Mining, University of Tehran, Iran. Pyrite powder was nanosized by a high-energy planetary ball mill method (Model Two cups, Amin Asia Company, Iran) [12]. Next, the rotation speeds of small and large Teflon cups were considered to be 300 and 160 rpm, respectively. The ratio of ball mass to powder mass was 10: 1, and pyrite nanosizing was completed in 6 h. Finally, the obtained powder was washed with distilled water to remove impurities and dried at 30 °C.

Sono-Fenton system

A glass container with a useful volume of 200 mL was applied as a sono-Fenton reactor. This reactor was equipped with a digital ultrasonic homogenizer (Model UP200St, Hielscher, Germany. Volume 2.0 L, output power 200 W, and frequency 26 kHz). The sonotrode of the sonicator was titanium (tip diameter = 7 mm).

Experimental

The TC stock solution was prepared by adding 0.05 g TC pure powder to 100 mL deionized water. Then, predetermined concentrations of TC (8.0-32 mg/L) were made from the stock solution. Sulfuric acid (1.0 M) and sodium hydroxide (1.0 M) were used to change the solution pH. The pH measurement was done through a digital pH meter (AZ 8686, Taiwan). To investigate the effect of oxidant and catalyst, HP and nano-pyrite were added to the samples in amounts of 1.0 to 4.0 mM and 0.2 to 1.0 g/L, respectively. Moreover, nano-pyrite was separated from the solution by centrifugation to perform catalyst recovery tests. All experiments were repeated three times and the average data were considered as results.

Analysis

TC concentration was measured by a UV-visible spectrophotometer at 365 nm (Model DR/5000, HACH, Germany) [20]. The measurement of aqueous Fe^{2+} was conducted by the spectrophotometric 1, 10-phenanthroline method at 510 nm.

TC removal efficiency was calculated according to the following equation:

$$\text{TC removal}(\%) = \frac{\text{TC}_0 - \text{TC}_t}{\text{TC}_0} \times 100 \quad (9)$$

Where TC_0 and TC_t represent the initial and residual TC concentrations (mg/L) in the solution, respectively.

The TC removal rate constant was calculated according to the following first-order kinetic equation:

$$\ln\left(\frac{\text{TC}_t}{\text{TC}_0}\right) = -kt \quad (10)$$

Where k is the rate constant (min^{-1}) and t is the reaction time (min).

Characterization of the nano-pyrite structure was done by X-ray powder diffraction (XRD, Model PW1730, PHILIPS, Holland) analysis with copper radiation at a scan rate of 2θ with a range of $10\text{--}80^\circ$ ($\lambda = 1.54056 \text{ \AA}$, $V = 40 \text{ kV}$, and $I = 30 \text{ mA}$). Moreover, functional groups of nano-pyrite were identified by Fourier transform infrared spectroscopy analysis (FTIR, Model AVATAR, Thermo, USA). Besides, energy-dispersive X-ray spectroscopy (EDX) and field emission scanning electron microscopy (FE-SEM, MIRA 3 TESCAN, Czech Republic) analyses were used to determine the chemical composition and morphology of nano-pyrite, respectively. Finally, Digimizer and Origin software was applied to plot the size distribution of synthesized nano-pyrite particles.

RESULTS AND DISCUSSION

Nano-pyrite characterization

The XRD patterns of pyrite and nano-pyrite are presented in Fig. 1a. Accordingly, peaks at 2 theta positions of 28.65° , 33.25° , 37.35° , 40.85° , 47.6° , 56.45° , 59.15° , 61.45° and 64.55° corresponding to the primary pyrite sample were recorded, which were completely consistent with the JPCDS no: 42-1340 crystal structure of pure pyrite [4]. Similarly, the distinct peaks appearing in the XRD diagram of the synthesized nano-pyrite confirmed the preservation of the pure pyrite crystal structure in the sample (22.95° , 28.35° , 31.25° , 32.7° , 35.35° , 36.8° , 38.95° , 40.6° , 47.05° , 53.4° , 56.3° , 58.75° , 61.45° , and 64.1°). According to the data, the crystal structure of the synthesized nano-pyrite was cubic and its nature was preserved after the nano process.

The functional groups and chemical bonds of nano-pyrite and pyrite were presented in the

FTIR diagram (Fig. 1b). In this way, S-O (1141 cm^{-1}), O-H (3429 cm^{-1}), Fe-O-OH (1024 cm^{-1}), Fe-S (831 cm^{-1}), and Fe-SO₄ (1633 cm^{-1}) [21, 22] were observed in the pyrite sample. In addition, 660 and 623 cm^{-1} absorption bands associated with the sulfur group were found in the analysis of the nano-pyrite catalyst. Besides, peak values of 1254 , 2926 , 1131 and 592 cm^{-1} were recorded in the nano-pyrite which related to O-C, C-H, S-O, and Fe-S groups, respectively [23].

According to the FE-SEM images, the fabricated nano-pyrite had nanoscale particles with regular structure morphology (Fig. 1c). The output data from EDX analysis showed that iron and sulfur were the main constituents of the synthesized nano-catalyst (Fig. 1d). Accordingly, Fe and S were included in 47.64% and 52.36% of nano-pyrite weight, respectively. It should be noted that Fe and S constituted 28.36% and 28.77% of the weight percentage of pyrite nanoparticle samples in the previous Fenton base studies, respectively [22, 23].

Analysis of the size distribution of synthesized nano-pyrite particles by Digimizer software (Fig. 1e) showed that most of the particles were less than 80 nm in size ($10\text{--}20 \text{ nm}$: 10% , $20\text{--}40 \text{ nm}$: 46% , $40\text{--}60 \text{ nm}$: 34% , and $60\text{--}80 \text{ nm}$: 10%). This confirmed the effectiveness of the mechanical method of ball milling in the catalyst nanosizing.

The effect of solution pH

To investigate the effect of solution pH, the values of 3.0 , 5.0 , 7.0 , and 9.0 were considered (Fig. 2). TC removal efficiencies by sono-Fenton nano-pyrite/HP system under reaction conditions of 24 mg/L TC, 3.0 mM HP, 30 W US, 0.8 g/L nano-pyrite, and 20 min at pH of 3.0 , 5.0 , 7.0 , and 9.0 were 66.8% , 54.6% , 42.4% , and 37.8% , respectively. Acidic conditions ($\text{pH}=3.0$) were more effective in TC removal. This phenomenon can be explained by the lower stability of HP in alkaline conditions and the higher oxidation potential of hydroxyl radical at lower pH levels [24]. Besides, the oxidation of nano-pyrite and the release of ferrous ions from it occur better in acidic conditions [25]. The result of these interactions according to Eqs. (1), (2), and (5) led to more effective production of hydroxyl radical and subsequently TC removal. In contrast, the precipitation of Fe^{2+} and the production of metal hydroxides can be the possible reason for decreasing the efficiency of TC removal at alkaline pH levels [3, 26].

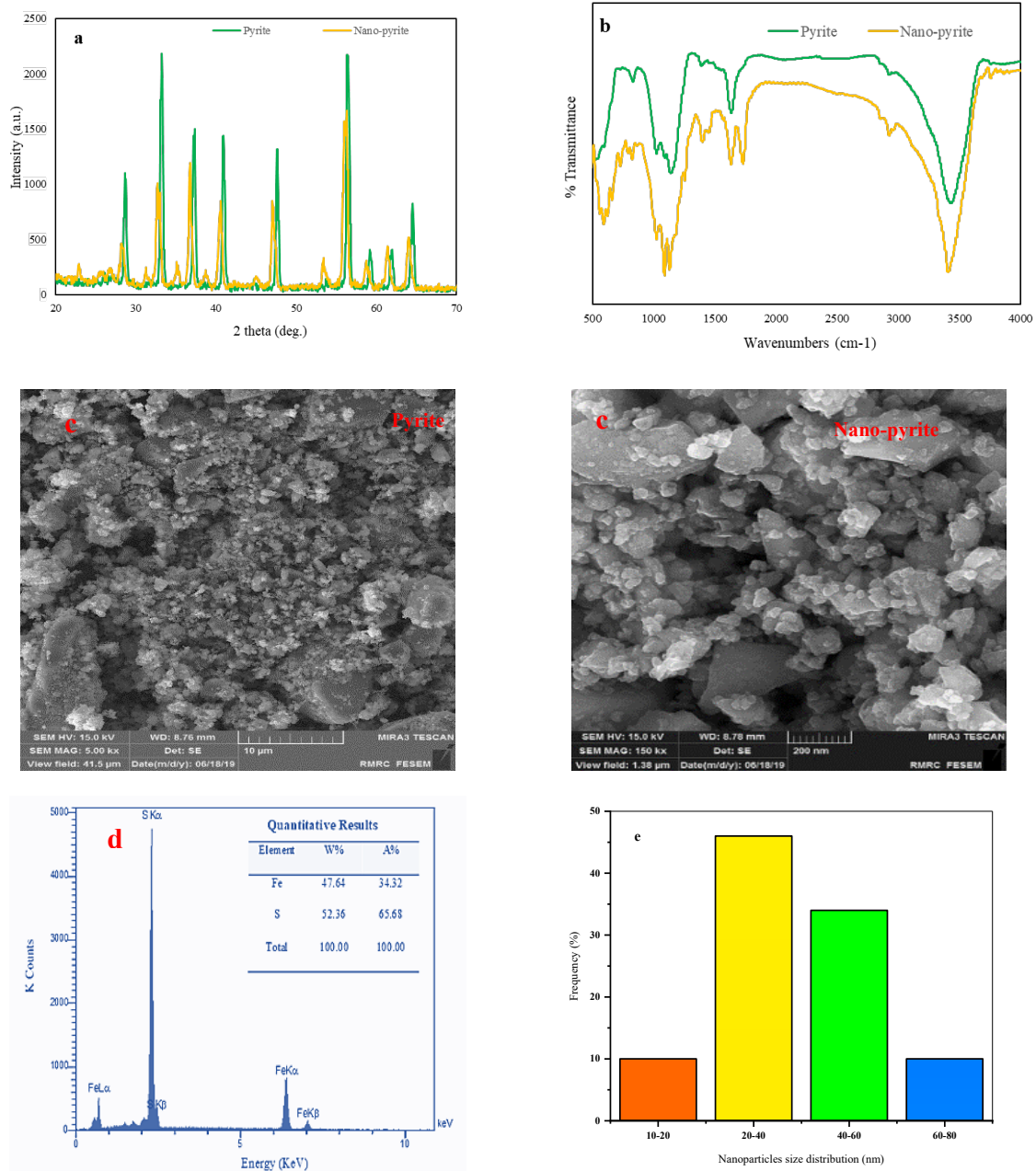


Fig. 1. Nano-pyrite characterization analyses. (a) XRD, (b) FTIR, (c) FE-SEM image, (d) EDX, and (e) particle size distribution

The effect of TC concentration

The effect of TC concentration was tested at initial values of 8.0, 16, 24, and 32 mg/L. Within 20 min, with the increase of TC concentration from 8.0 to 32 mg/L, the removal efficiency decreased by about 10% (Fig. 3). This means that the interference of by-products in the sono-Fenton nano-pyrite/HP system at high TC concentrations decreased the efficiency. Previous studies based on AOPs also confirmed this fact [27-29].

The effect of oxidant and nano-catalyst dosages

The effect of nano-catalyst and HP dosages on TC degradation is shown in Fig. 4. The results indicated an increase in TC removal efficiency in higher doses of nano-pyrite. It seems that the possible reason for this effect is the release of more ferrous ions in high amounts of nano-pyrite and the subsequent promotion of hydroxyl radical production. Therefore, 1 g/L of nano-pyrite was selected as the optimum dose of the process with



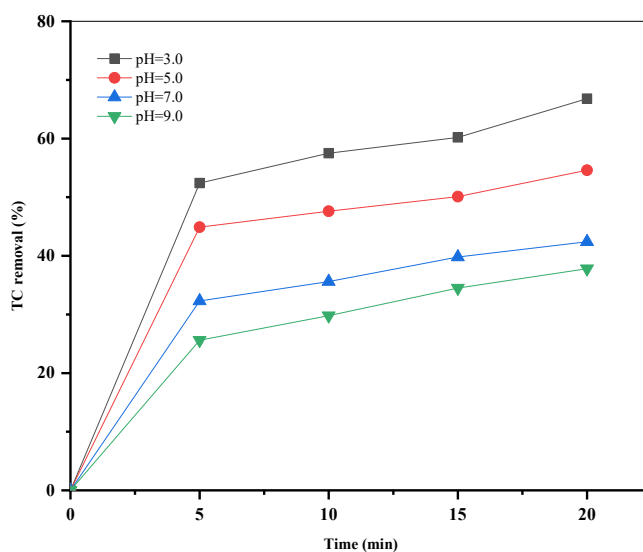


Fig. 2. The effect of pH solution on TC removal

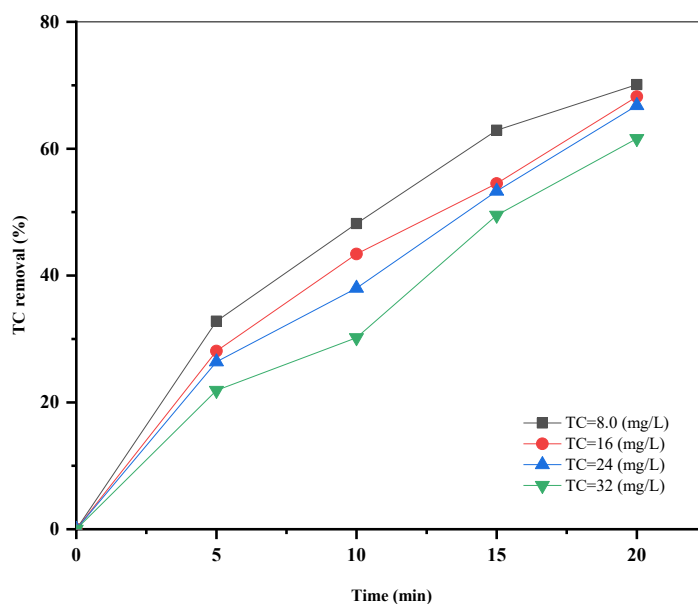


Fig. 3. The effect of initial TC concentration on removal efficiency

75.3% TC removal in 20 min. Similarly, increasing the concentration of HP led to an increase in TC removal, so that the highest removal efficiency (84.6%) was obtained at 4 mM HP. The presence of more HP in the solution provided a more ideal media for the formation of HO^\cdot by the Fenton-based processes. This is consistent with the results of our previous study [7].

The effect of US power

In the reaction conditions of pH 3.0, TC 8.0 mg/L, HP 4.0 mM, and nano-pyrite 1.0 g/L, the

effect of different powers of US was tested (Fig. 5). Within 20 min, TC removal efficiencies at 10, 20, 30, and 40 W were observed to be 77.7%, 81.2%, 84.6%, and 93.1%, respectively. As proven in previous studies, the oscillation and cavitation effects of US waves promote the degradation of organic pollutants [30-32]. Furthermore, the intensity of mixing by US waves at higher powers leads to better nano-catalyst solubility and mass transfer [33]. Therefore, in this study, a US power of 40 W was recorded as the optimal value.

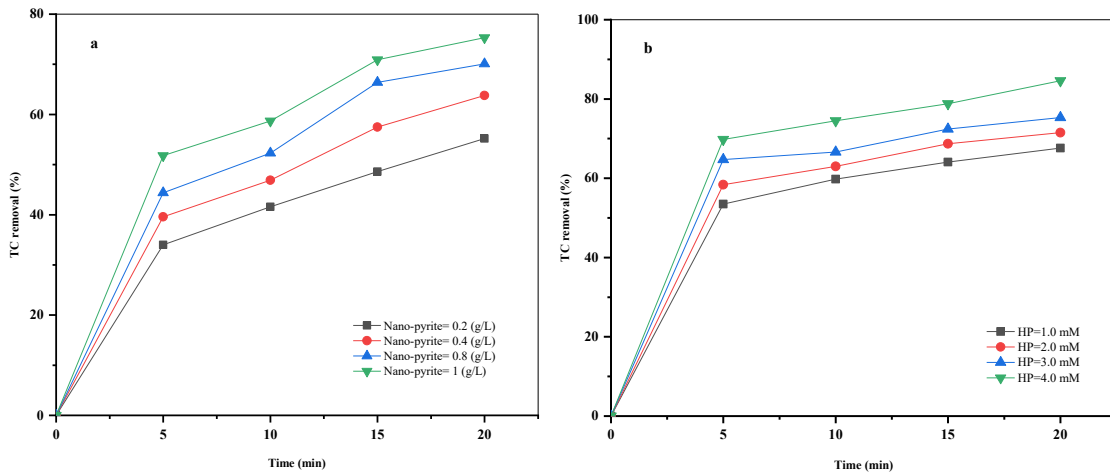


Fig. 4. The effect of nano-catalyst (a) and HP (b) dosages on TC removal

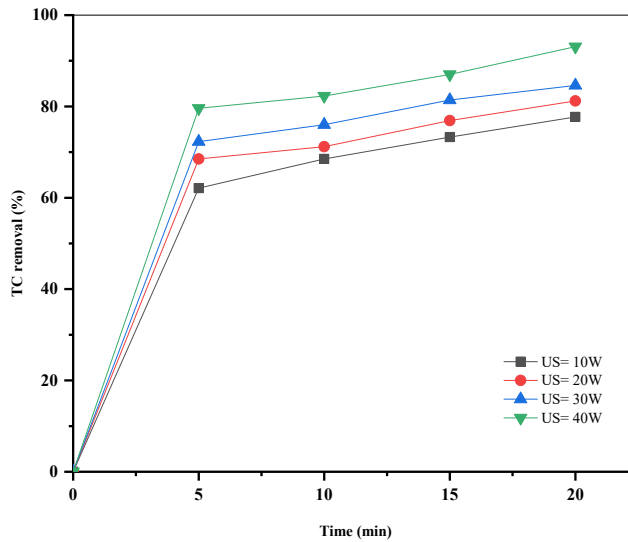
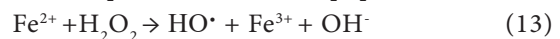
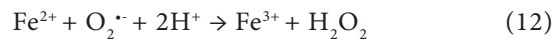


Fig. 5. The effect of US output power on TC removal

Comparison of TC removal in different systems

In the present study, the contribution of different components including nano-pyrite, HP, US, nano-pyrite/HP, and nano-pyrite/HP/US in TC removal under the same reaction conditions was compared (Fig. 6). At 20 min, nano-pyrite alone (1.0 g/L) removed 21.6% of TC. This amount of TC removal may be related to adsorption by nano-pyrite particles. In addition, nano-pyrite oxidation reactions (Eqs. (11-13)) produced TC oxidizing active agents such as superoxide and hydroxyl radicals.



In the next section, HP alone (4.0 mM) was added to the solution at the same time, which recorded 24.3% removal efficiency. Although HP removed the TC, its efficiency was not acceptable enough. The oxidant activation did not occur without nano-pyrite, and practically HP alone was not effective in TC removal. Next, the effectiveness of US power



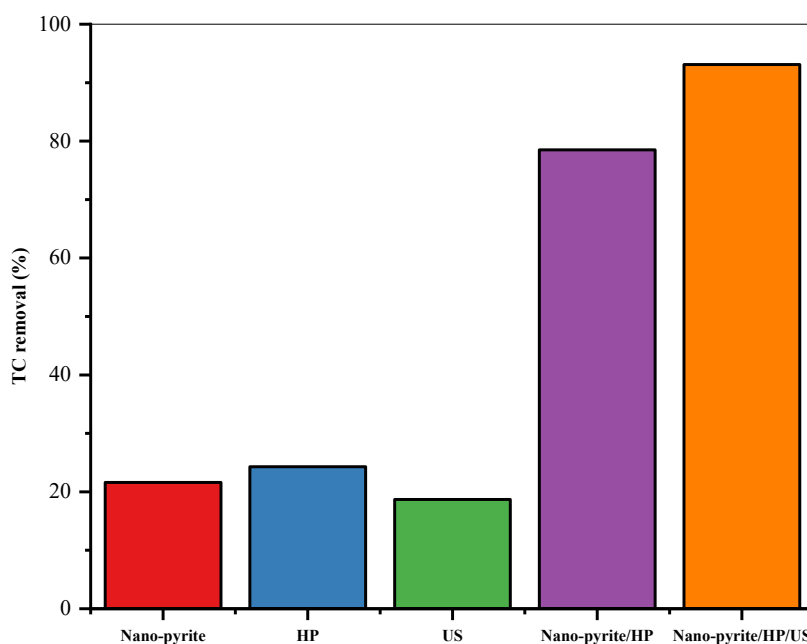


Fig. 6. Comparison of TC removal in different systems. Conditions: pH = 3.0, TC 8.0 mg/L, 40 W US, 1.0 g/L nano-pyrite, 4.0 mM HP and 20 min

in removal efficiency was tested. Accordingly, 18.7% TC was removed by 40 W US. Since the US waves decompose HP and generate hydroxyl radical, the removal efficiency can be attributed to this reason (Eq. 5). A significant increase in TC removal efficiency (78.5%) was recorded by nano-pyrite/HP system. Obviously, with the simultaneous presence of ferrous ion and HP in the bulk solution, the Fenton reaction occurred, and the hydroxyl radical caused the effective degradation of TC (Eq. 1). The enhancement of the removal efficiency was observed in the integrated system of nano-pyrite /HP/US with 93.1% TC removal. In other words, the synergy between sono-catalysis and Fenton reactions due to the simultaneous application of nano-pyrite, HP, and US power resulted in the highest TC removal rate. In addition to the above-mentioned reactions, the application of US forces to the nano-pyrite/HP system caused high turbulence, nano-catalyst fluidization, and mass transfer [14, 15, 34]. Meanwhile, the US irradiation with its oscillating effect cleaned the ferric hydroxide deposits formed on the nano-pyrite surface and contributed to the rapid and efficient removal of TC. These statements were consistent with the observations of previous studies Diao et al.'s study [16].

The effect of radical scavengers and the determination of process mechanism

To investigate the process mechanism, tert-butanol alcohol (3.0 mM) and methanol (3.0 mM) were added to the nano-pyrite/HP/US system under optimal conditions as HO^\bullet and $\text{SO}_4^{\bullet-}$ (sulfate radical) scavengers, respectively. The data showed that the TC removal efficiency in the presence of methanol was 54.2%, while the corresponding value in the presence of tert-butanol alcohol was 15.6% within 20 min. It can be concluded that the active oxidative species and the main agent of TC degradation in the process was HO^\bullet . As the proposed mechanism of the process, US waves with the property of turbulence and oscillation cause the release of more ferrous ions from nano-pyrite. This phenomenon leads to more effective production of hydroxyl radical in the presence of HP, which was the main factor of TC degradation. It has also been proven in previous studies that US mechanical waves clean the surface of the catalyst and improve its performance [16]. Moreover, TC degradation rates using the kinetic model of the first-order equation for different systems were presented in Table 1. Finally, the performance of sono/Fenton processes in the presence of different iron catalysts is compared in Table 2.

Table 1. TC degradation rate based on a kinetic model of the first-order equation

| Systems | pH | Initial TC (mg/L) | Time (min) | K (1/min) | Ln (TC _t /TC ₀) | R ² |
|-------------------|-----|-------------------|------------|-----------|--|----------------|
| Nano-pyrite | 3.0 | 8.0 | 20 | 0.0121 | - 0.243 | 0.9914 |
| HP | 3.0 | 8.0 | 20 | 0.0139 | - 0.278 | 0.9916 |
| US | 3.0 | 8.0 | 20 | 0.0103 | - 0.207 | 0.9954 |
| Nano-pyrite/HP | 3.0 | 8.0 | 20 | 0.0768 | - 1.53 | 0.9974 |
| Nano-pyrite/HP/US | 3.0 | 8.0 | 20 | 0.133 | - 2.673 | 0.9418 |

Table 2. Performance of sono/Fenton processes with different catalysts in organic pollutant removal

| Pollutant | Pollutant concentration (mg/L) | Catalyst | pH | HP concentration | Time (min) | US power (W) | Removal rate (%) | Ref |
|-------------------|--------------------------------|------------------|-----|------------------|------------|--------------|------------------|-----------|
| Reactive Blue 181 | 50 | Ferrous ion | 3.0 | 40 mg/L | 30 | 90 | 93.5 | [35] |
| Acid orange 7 | 200 | Zero-valent iron | 3.0 | 5.0 mM | 30 | 201 | 90 | [36] |
| Phenol | 200 | Ferrous ion | 3.0 | 800 mg/L | 60 | 120 | 72 | [37] |
| RY 145 + PVA | 150 | Ferrous ion | 3.0 | 15 mg/L | 60 | 80 | 95 | [38] |
| TC | 8.0 | Nano-pyrite | 3.0 | 4.0 mM | 20 | 40 | 93.1 | This Work |

Recyclability and stability of the nano-pyrite catalyst

Fig. 7 shows the stability and recyclability of synthesized nano-pyrite under optimum conditions of the Sono/Fenton process. In this way, the nano-pyrite was tested in four consecutive runs. The results showed that the TC removal efficiency from the first to the fourth run reached 93.1% to 70.3%. This means that the recyclability of nano-pyrite has been very successful. Besides, the amount of iron leached from nano-pyrite was investigated during recyclability. Accordingly, the concentration of aqueous ferrous ions reached 8.2 mg/L at the end of the fourth run. Indeed, the ferrous ion supplied from nano-pyrite was sufficient for the Fenton reaction even after four recoveries.

Determination of TC degradation intermediates

To determine the by-products of TC degradation in the proposed system, liquid chromatography-mass spectroscopy (LC-MS) device was used. Under optimal conditions, intermediates including malealdehyde, phenol, carboxylic acids, maleic acid, formic acid, and oxalic acid were identified in the solution. It is concluded that TC degradation in the nano-pyrite/HP/US system was complete due to the formation of low-weight molecules and simple organic acids.

CONCLUSIONS

The promotion of TC degradation through the combined system with the simultaneous participation of nano-pyrite and HP under ultrasound irradiation was studied. Within 20 min, the proposed sono-Fenton system degraded 93.1% of TC in an aqueous medium. In this way, except for the initial concentration of TC and pH, TC removal efficiency was increased by increasing the operating parameters (HP and catalyst dosages, US power, and time). Characterization analysis, especially Digimizer software, confirmed that the synthesized catalyst was nanosized. Accordingly, the size of all nano-pyrite particles was less than 80 nm. In summary, nano-pyrite, HP, and US waves caused synergy in promoting TC removal through their catalytic, oxidizing, and oscillatory functions, respectively.

ABBREVIATIONS

| | |
|-------|---|
| AOPs | Advanced oxidation processes |
| EDX | Energy-dispersive X-ray spectroscopy |
| HP | Hydrogen peroxide |
| FTIR | Fourier-transform infrared spectroscopy |
| LC-MS | Liquid chromatography-mass spectroscopy |



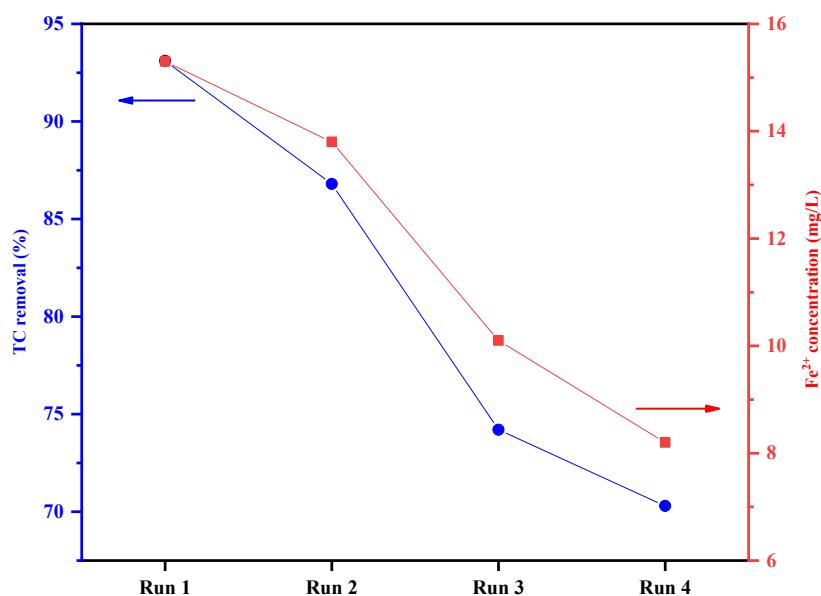


Fig. 7 Recyclability and ferrous ion concentration produced from nano-pyrite in consecutive runs. Conditions: pH = 3.0, TC 8.0 mg/L, 40 W US, 1.0 g/L nano-pyrite, 4.0 mM HP and 20 min

| | |
|-----|------------------------------|
| SEM | Scanning electron microscopy |
| TC | Tetracycline |
| US | Ultrasound |
| XRD | X-ray powder diffraction |

REFERENCES

- [1]. Zhou J, Ma F, Guo H, Su D. Activate hydrogen peroxide for efficient tetracycline degradation via a facile assembled carbon-based composite: synergism of powdered activated carbon and ferrous oxide nanocatalyst. *Applied Catalysis B: Environmental*. 2020;269:118784. <https://doi.org/10.1016/j.apcatb.2020.118784>
- [2]. Zhu X-D, Wang Y-J, Sun R-J, Zhou D-M. Photocatalytic degradation of tetracycline in aqueous solution by nanosized TiO₂. *Chemosphere*. 2013;92(8):925-32. <https://doi.org/10.1016/j.chemosphere.2013.02.066>
- [3]. Aseman-Bashiz E, Rezaee A, Moussavi G. Ciprofloxacin removal from aqueous solutions using modified electrochemical Fenton processes with iron green catalysts. *Journal of Molecular Liquids*. 2021;324:114694. <https://doi.org/10.1016/j.molliq.2020.114694>
- [4]. Aseman-Bashiz E, Sayyaf H. Synthesis of nano- FeS₂ and its application as an effective activator of ozone and peroxydisulfate in the electrochemical process for ofloxacin degradation: A comparative study. *Chemosphere*. 2021;274:129772. <https://doi.org/10.1016/j.chemosphere.2021.129772>
- [5]. Chen Z, Wang L, Xu H, Wen Q. Efficient heterogeneous activation of peroxymonosulfate by modified CuFe₂O₄ for degradation of tetrabromobisphenol A. *Chemical Engineering Journal*. 2020;389:124345. <https://doi.org/10.1016/j.cej.2020.124345>
- [6]. Colades JI, Huang C-P, Retumban JD, Garcia-Segura S, de Luna MDG. Electrochemically-driven dosing of iron (II) for autonomous electro-Fenton processes with in situ generation of . *Journal of Electroanalytical Chemistry*. 2020;856:113639. <https://doi.org/10.1016/j.jelechem.2019.113639>
- [7]. Aseman-Bashiz E, Sayyaf H. Metformin degradation in aqueous solutions by electro-activation of persulfate and hydrogen peroxide using natural and synthetic ferrous ion sources. *Journal of Molecular Liquids*. 2020;300:112285. <https://doi.org/10.1016/j.molliq.2019.112285>
- [8]. Ghanbari F, Moradi M. A comparative study of electrocoagulation, electrochemical Fenton, electro-Fenton and peroxi-coagulation for decolorization of real textile wastewater: electrical energy consumption and biodegradability improvement. *Journal of Environmental Chemical Engineering*. 2015;3(1):499-506. <https://doi.org/10.1016/j.jece.2014.12.018>
- [9]. Devlin TR, Kowalski MS, Pagaduan E, Zhang X, Wei V, Oleszkiewicz JA. Electrocoagulation of wastewater using aluminum, iron, and magnesium electrodes. *Journal of hazardous materials*. 2019;368:862-8. <https://doi.org/10.1016/j.jhazmat.2018.10.017>
- [10]. Diao Z-H, Xu X-R, Jiang D, Li G, Liu J-J, Kong L-J, et al. Enhanced catalytic degradation of ciprofloxacin with FeS₂/SiO₂ microspheres as heterogeneous Fenton catalyst: kinetics, reaction pathways and mechanism. *Journal of hazardous materials*. 2017;327:108-15. <https://doi.org/10.1016/j.jhazmat.2016.12.045>
- [11]. Zheng X, Niu X, Zhang D, Lv M, Ye X, Ma J, et al. Metal-based catalysts for persulfate and peroxymonosulfate activation in heterogeneous ways: A review. *Chemical Engineering Journal*. 2022;429:132323. <https://doi.org/10.1016/j.cej.2021.132323>
- [12]. Aseman-Bashiz E, Rezaee A, Moussavi G. Effective removal of hexavalent chromium using microbial cellulose/polyaniline cathode and nanosized FeS₂ in the form of an integrated electrochemical system. *Journal of Water Process*

- Engineering. 2021;44:102333.
<https://doi.org/10.1016/j.jppe.2021.102333>
- [13]. Song B, Zeng Z, Almatrafi E, Shen M, Xiong W, Zhou C, et al. Pyrite-mediated advanced oxidation processes: Applications, mechanisms, and enhancing strategies. *Water Research*. 2022;118048.
<https://doi.org/10.1016/j.watres.2022.118048>
- [14]. Zhang T, Yang Y, Li X, Yu H, Wang N, Li H, et al. Degradation of sulfamethazine by persulfate activated with nanosized zero-valent copper in combination with ultrasonic irradiation. *Separation and Purification Technology*. 2020;239:116537.
<https://doi.org/10.1016/j.seppur.2020.116537>
- [15]. Gao Y-q, Gao N-y, Wang W, Kang S-f, Xu J-h, Xiang H-m, et al. Ultrasound-assisted heterogeneous activation of persulfate by nano zero-valent iron (nZVI) for the propranolol degradation in water. *Ultrasonics sonochemistry*. 2018;49:33-40.
<https://doi.org/10.1016/j.ultsonch.2018.07.001>
- [16]. Diao Z-H, Lin Z-Y, Chen X-Z, Yan L, Dong F-X, Qian W, et al. Ultrasound-assisted heterogeneous activation of peroxymonosulfate by natural pyrite for 2, 4-dichlorophenol degradation in water: Synergistic effects, pathway and mechanism. *Chemical Engineering Journal*. 2020;389:123771.
<https://doi.org/10.1016/j.cej.2019.123771>
- [17]. Asaithambi P, Govindarajan R, Yesuf MB, Selvakumar P, Alemayehu E. Enhanced treatment of landfill leachate wastewater using sono (US)-ozone (O₃)-electrocoagulation (EC) process: role of process parameters on color, COD and electrical energy consumption. *Process Safety and Environmental Protection*. 2020;142:212-8.
<https://doi.org/10.1016/j.psep.2020.06.024>
- [18]. Yin R, Guo W, Wang H, Du J, Zhou X, Wu Q, et al. Enhanced peroxymonosulfate activation for sulfamethazine degradation by ultrasound irradiation: performances and mechanisms. *Chemical Engineering Journal*. 2018;335:145-53.
<https://doi.org/10.1016/j.cej.2017.10.063>
- [19]. Sayadi MH, Chamanehpour E, Fahoul N. The ultrasonic process with titanium magnetic oxide nanoparticles to enhance the amoxicillin removal efficiency. *Journal of Water and Environmental Nanotechnology*. 2022;7(3):241-51.
- [20]. Jafari AJ, Kakavandi B, Jaafarzadeh N, Kalantary RR, Ahmadi M, Babaei AA. Fenton-like catalytic oxidation of tetracycline by AC@ Fe₃O₄ as a heterogeneous persulfate activator: adsorption and degradation studies. *Journal of Industrial and Engineering Chemistry*. 2017;45:323-33.
<https://doi.org/10.1016/j.jiec.2016.09.044>
- [21]. Venkateshalu S, Kumar PG, Kollu J, Jeong SK, Grace AN. Solvothermal synthesis and electrochemical properties of phase pure pyrite FeS₂ for supercapacitor applications. *Electrochimica Acta*. 2018;290:378-89.
<https://doi.org/10.1016/j.electacta.2018.09.027>
- [22]. Fathinia S, Fathinia M, Rahmani AA, Khataee A. Preparation of natural pyrite nanoparticles by high energy planetary ball milling as a nanocatalyst for heterogeneous Fenton process. *Applied Surface Science*. 2015;327:190-200.
<https://doi.org/10.1016/j.apsusc.2014.11.157>
- [23]. Khataee A, Fathinia S, Fathinia M. Production of pyrite nanoparticles using high energy planetary ball milling for sonocatalytic degradation of sulfasalazine. *Ultrasonics sonochemistry*. 2017;34:904-15.
<https://doi.org/10.1016/j.ultsonch.2016.07.028>
- [24]. Barhoumi N, Oturan N, Olvera-Vargas H, Brillas E, Gadri A, Ammar S, et al. Pyrite as a sustainable catalyst in electro-Fenton process for improving oxidation of sulfamethazine. Kinetics, mechanism and toxicity assessment. *Water Research*. 2016;94:52-61.
<https://doi.org/10.1016/j.watres.2016.02.042>
- [25]. Diao Z-H, Liu J-J, Hu Y-X, Kong L-J, Jiang D, Xu X-R. Comparative study of Rhodamine B degradation by the systems pyrite/ and pyrite/persulfate: reactivity, stability, products and mechanism. *Separation and Purification Technology*. 2017;184:374-83.
<https://doi.org/10.1016/j.seppur.2017.05.016>
- [26]. Mirzaei A, Chen Z, Haghghat F, Yerushalmi L. Removal of pharmaceuticals from water by homo/heterogeneous Fenton-type processes-A review. *Chemosphere*. 2017;174:665-88.
<https://doi.org/10.1016/j.chemosphere.2017.02.019>
- [27]. Zhong Y, Shih K, Diao Z, Song G, Su M, Chen D, et al. Peroxymonosulfate activation through LED-induced ZnFe₂O₄ for levofloxacin degradation. *Chemical Engineering Journal*. 2021;417:129225.
<https://doi.org/10.1016/j.cej.2021.129225>
- [28]. Ouyang D, Yan J, Qian L, Chen Y, Han L, Su A, et al. Degradation of 1, 4-dioxane by biochar supported nano magnetite particles activating persulfate. *Chemosphere*. 2017;184:609-17.
<https://doi.org/10.1016/j.chemosphere.2017.05.156>
- [29]. Cao J, Lai L, Lai B, Yao G, Chen X, Song L. Degradation of tetracycline by peroxymonosulfate activated with zero-valent iron: performance, intermediates, toxicity and mechanism. *Chemical Engineering Journal*. 2019;364:45-56.
<https://doi.org/10.1016/j.cej.2019.01.113>
- [30]. Steter JR, Barros WR, Lanza MR, Motheo AJ. Electrochemical and sonoelectrochemical processes applied to amaranth dye degradation. *Chemosphere*. 2014;117:200-7.
<https://doi.org/10.1016/j.chemosphere.2014.06.085>
- [31]. Najafi M, Bastami TR, Binesh N, Ayati A, Emamverdi S. Sono-sorption versus adsorption for the removal of congo red from aqueous solution using NiFeLDH/Au nanocomposite: Kinetics, thermodynamics, isotherm studies, and optimization of process parameters. *Journal of Industrial and Engineering Chemistry*. 2022;116:489-503.
<https://doi.org/10.1016/j.jiec.2022.09.039>
- [32]. Bastami TR, Khaknahad S, Malekshahi M. Sonochemical versus reverse-precipitation synthesis of Cu₂O/ /MoC nano-hybrid: removal of reactive dyes and evaluation of smartphone for colorimetric detection of organic dyes in water media. *Environmental Science and Pollution Research*. 2020;27(9):9364-81.
<https://doi.org/10.1007/s11356-019-07368-0>
- [33]. Pang Y, Ruan Y, Feng Y, Diao Z, Shih K, Chen D, et al. Ultrasound assisted zero valent iron corrosion for peroxymonosulfate activation for Rhodamine-B degradation. *Chemosphere*. 2019;228:412-7.
<https://doi.org/10.1016/j.chemosphere.2019.04.164>
- [34]. Omrani E, Ahmadpour A, Heravi M, Bastami TR. Novel ZnTi LDH/h-BN nanocomposites for removal of two different organic contaminants: Simultaneous visible light photodegradation of Amaranth and Diazepam. *Journal of*



- Water Process Engineering. 2022;47:102581.
<https://doi.org/10.1016/j.jwpe.2022.102581>
- [35].Basturk E, Karatas M. Advanced oxidation of reactive blue 181 solution: A comparison between fenton and sono-fenton process. Ultrasonics sonochemistry. 2014;21(5):1881-5.
<https://doi.org/10.1016/j.ultsonch.2014.03.026>
- [36].Zhang H, Zhang J, Zhang C, Liu F, Zhang D. Degradation of CI Acid Orange 7 by the advanced Fenton process in combination with ultrasonic irradiation. Ultrasonics sonochemistry. 2009;16(3):325-30.
<https://doi.org/10.1016/j.ultsonch.2008.09.005>
- [37].Arjunan B, Karuppan M. Degradation of phenol in aqueous solution by Fenton, sono-Fenton and sono-photo-Fenton methods. Clean-Soil, Air, Water. 2011;39(2):142-7.
<https://doi.org/10.1002/clen.201000072>
- [38].Özdemir C, Öden MK, Şahinkaya S, Kalipçi E. Color removal from synthetic textile wastewater by sono fenton process. Clean-Soil, Air, Water. 2011;39(1):60-7.
<https://doi.org/10.1002/clen.201000263>